SUPPLEMENTAL METHODS

Animals and Surgery:

β-catenin floxed transgenic mice with loxP sites flanking Exons 2-6 were bred to liver-specific albumin-cre (Alb-cre) mice (both in C57BL/6 background), and the resulting offspring carrying a floxed and WT allele are then backcrossed to floxed-homozygous animal to obtain a conditional KO. A total of 8 KO and 8 littermate controls of both sexes were used for BDL. Mice were sacrificed at 14 days after surgery, or at various earlier time points (4 hour, 1 day, 2 days) as indicated. Blood samples were collected from the orbital sinus at the time of sacrifice. Serum biochemical measurements for total bilirubin, conjugated bilirubin, alkaline phosphatase (ALP), aspartate aminotransferase (AST), alanine aminotransferase (ALT), and gamma glutamyl transpeptidase (GGTP) were performed by the University of Pittsburgh Medical Center Clinical Chemistry laboratory.

β-catenin KO and corresponding controls ($n \geq 3$) were administered 0.1% DDC diet as described previously (1). Mice were sacrificed after 1 month of diet, and livers harvested for subsequent analysis as described below.

GW4064 (Tocris Bioscience, Bristol, United Kingdom) was administered to fasting WT and β-catenin KO mice intraperitoneally at a concentration of 30mg/kg (2, 3). Animals were sacrificed 1 hour and 3 hours after treatment. WT and β-catenin KO livers were also harvested at baseline for multiple biochemical,

molecular, and histochemical analyses (see below). Livers from whole-body FXR KO mice (on a C57BL/6 background) (4) were kindly provided by Dr. Grace Guo, Rutgers University.

Measurement of liver bile acids:

Liver total BA were measured using a total bile acids kit from Diazyme (Poway, CA) or Crystal Chem (Downers Grove, IL), as per the manufacturer's instructions. For the Diazyme kit, frozen liver tissue was homogenized in either ice-cold phosphate-buffered saline with Halt protease and phosphatase inhibitor cocktail (Pierce, Rockford, IL) and centrifuged at 600*g* for 10 minutes at 4°C to remove debris. The supernatant was then centrifuged at 105,000*g* at 4°C to recover purified cytosol. Cytosolic total bile acid levels were measured and normalized to protein concentration for each sample. For the Crystal Chem kit, frozen liver tissue was homogenized in 70% ethanol at room temperature and then incubated in tightly capped glass tubes at 50°C for 2 hours. The homogenates were centrifuged at 6,000*g* for 10 minutes to remove debris. Total bile acid levels were measured and concentrations determined using the calibration curve and mean change in absorbance value for each sample.

Transient transfection and luciferase assay:

The Hep3B human hepatoma cell line, which was obtained from ATCC, Manassas, VA, was transfected and measured for luciferase activity as previously described (5). Briefly, Hep3Bs grown in Eagle's Minimal Essential

Medium (American Type Culture Collection, Manassas, VA) with 10% FBS (Atlanta Biologicals, Lawrenceville, GA) were seeded onto 6-well plates and transiently transfected with plasmids or siRNA combined with reporters as indicated. Validated human β-catenin (CTNNB1) siRNA or negative control siRNA 1 (Ambion, Inc., Austin, TX) was used at a final concentration of 25 nM in the presence of Lipofectamine 2000 reagent (Invitrogen, Carlsbad, CA), as per the manufacturer's instructions. Simultaneously, either 0.8 μg of TOPflash reporter plasmid (which specifically measures β-catenin/Tcf-dependent transcriptional activation; Upstate Biotechnology) or 0.2 μg of pGL4-TK luciferase reporter plasmid specific for SHP activity (provided by Dr. Grace Guo (6)) was co-transfected with 0.1 μg of Renilla plasmid, also in the presence of Lipofectamine 2000. Where indicated, cells were treated with 1 μM GW4064 or vehicle control 5 hours after transfection. The media was changed 24 hours after transfection and fresh GW4064 or vehicle was added to the appropriate wells. The cells were harvested 48 hours after transfection for protein extraction and luciferase assay. Luciferase assays were performed using the Dual Luciferase Assay System kit, in accordance with the manufacturer's protocols (Promega, Madison, WI). Relative luciferase activity (in arbitrary units) was reported as fold induction after normalization to Renilla for transfection efficiency.

For drug treatments, Hep3B cells were transfected with Renilla and either SHP luciferase reporter plasmid as described above. After 5 hours, fresh media containing either vehicle control or ICG-001 (developed and provided by Dr.

Michael Kahn) at a final concentration of 10μM, was added to the cells, simultaneous with addition of 1 μM GW4064 or vehicle control (7). The media was changed 24 hours after transfection and fresh ICG-001, GW4064, and/or vehicle control was added to the wells. Cells were harvested 48 hours after transfection for luciferase assays, which were performed as described above.

Use of control plasmid or plasmid expressing a constitutively active form of β-catenin, which is mutated at serine 33 to tyrosine (S33Y), was recently described (8). The cells were co-transfected at a concentration of 1.2 μg with SHP or TOPflash reporters. Cells were harvested for luciferase assay 48 hours after transfection as described above.

Finally, Hep3B cells in 100mm dishes (n=2 dishes per condition) were treated with vehicle control or GW4064 as described above, or transfected with either control, β-catenin, or RXRα siRNA, or pcDNA, S33Y β-catenin, or RXRα overexpression plasmid (provided by Dr. Grace Guo), and harvested 48 hours after treatment or transfection for protein extraction and immunoprecipitation as described below.

Chromatin immunoprecipitation:

Freshly harvested liver (T0 and 14 days post-BDL; WT and β-catenin KO; n=3 each genotype/time point) was finely minced on ice and added to PBS containing 1% formaldehyde, 0.1M PMSF, 0.5M EDTA, and Halt inhibitor cocktail.

Alternatively, Hep3B cells transfected with either control or β-catenin siRNA (with or without GW4064), or pcDNA or S33Y β-catenin plasmids, were harvested from 100mm dishes (n=3 per condition) with the same PBS plus additive solution above. Tissues or cells were cross-linked for 15 minutes on a rotator at room temperature, followed by quenching with 0.125 M glycine and rinsing with cold PBS. Tissues or cells were then collected and homogenized in cold PBS plus additives with a Wheaton overhead homogenizer. After pelleting, cells from tissue or cell culture were lysed in 5Mm PIPES (pH 8.0), 85mM KCl, and 0.5% NP-40 using a Dounce homogenizer and incubated on ice for 15 minutes to release nuclei. Nuclei were resuspended in 50 mM Tris, pH 8.1, 10 mM EDTA, 1%SDS, and inhibitors at 5X the cell volume and incubated on ice for 20 minutes, then sonicated with a Bioruptor at 10 minute intervals until chromatin fragments were 200-500bp in length. At this point 25µl of the chromatin was removed and saved as input. Chromatin aliquots were diluted in IP dilution buffer and precleared with Protein G-Sepharose beads (GE Healthcare, Pittsburgh, PA) for 3 hours at 4 °C. Supernatants were incubated overnight at 4°C with 10µg of either RXRα antibody (sc-774X; Santa Cruz), FXR antibodies (rabbit FXR sc-13063X and goat FXR sc-1204X; 5µg each; Santa Cruz), CAR antibody (sc-13065; Santa Cruz); TCF4 antibody (C9B9 clone; Cell Signaling), or H4K5Ac (39699; Active Motif, Carlsbad, CA). Antibody-chromatin complexes were recovered by incubation with Protein G-Sepharose for 3 hours at 4°C and then centrifuged. Additional IP buffer was added to each sample, and then samples were loaded onto a ChIP filtration column (CHIP-IT High Sensitivity Kit; Active

Motif, Carlsbad, CA) and gravity filtered, followed by washing and elution by centrifugation. Samples were de-crosslinked by incubation with Proteinase K at 55°C for 30 min then followed by 80°C for 2 hours, then purified with the MiniElute kit (Qiagen).

The resulting DNA fragments and input controls were subjected to real-time PCR as described above using primer sets listed in Supplemental Tables 3 and 4. Results in Figure 6 (ChIP on Hep3B cells treated with siRNAs or expression plasmids) represent pooled samples from n≥3 plates per treatment group assayed in triplicate, while results in Supplemental Figure 5 represent the average of three individual samples per time point per genotype assayed in triplicate (representative results from n=2 independent experiments are shown). ChIP q-PCR data was normalized to percent input for each sample, and then normalized to the corresponding control (for liver tissues: WT baseline; for Hep3B cells: cells treated with pcDNA plasmid alone or siRNA plus DMSO) to determine fold change.

Histology and Immunohistochemistry:

Liver tissue fixed in 10% formalin and embedded in paraffin was sectioned 4 μm in thickness and assessed for histological changes by hematoxylin and eosin (H&E) staining. Biliary infarcts were quantified in liver sections from KO (n=8) and WT (n=8) at 14 days of BDL. Bile infarcts were counted in an entire H&E section

at 100x, representing part of a lobe from each BDL-subjected KO and WT animal and compared for statistical differences by student t test.

Immunohistochemistry (IHC) on paraffin-embedded sections of mouse livers was performed on 4 μm thick tissue sections, which were microwaved or steamed in citrate buffer, pretreated with 3% H_2O_2, and blocked using Ultra V Block (Lab Vision Products, Fremont, CA). Primary antibodies used for this project were anti-β-catenin (1:150), anti-smooth muscle actin (1:200), anti-CK19 (1:10), anti-FXR (1:25), and anti-CD45 (1:100; all from Santa Cruz Biotechnology, Santa Cruz, CA). All primary antibodies were incubated for 1 hour. Secondary antibodies were biotinylated horse anti-mouse (Vector Laboratories, Inc., Burlingame, CA) or biotinylated goat anti-rabbit (Chemicon, Temecula, CA), used at 1:500 dilution. Immunohistochemistry was performed using the Vectastain ABC Elite kit (Vector Laboratories, Inc., Burlingame, CA) and developed using DAB (Vector Laboratories, Inc., Burlingame, CA). The slides were counterstained with Shandon's hematoxylin (Thermo Fisher).

For detection of fibrosis, sections were rehydrated and placed in Sirius Red staining solution for 1 h at room temperature. Sections were washed with acidified water, dehydrated, and coverslipped. Apoptosis was determined using terminal deoxynucleotidyl transferase dUTP nick-end labeling (TUNEL) staining (ApopTag Peroxidase in Situ Apoptosis Detection Kit, Millipore, Temecula, CA, USA). To assess neutrophil accumulation, liver sections were stained using a

Naphthol-ASD Chloroacetate Esterase Kit (Sigma, St. Louis, MO), as per the manufacturer's instructions.

Immunofluorescence:

A6 immunofluorescence was performed as previously described (9). Briefly, frozen sections were fixed in ice cold acetone for 10 minutes, washed in phosphate-buffered saline (PBS), and incubated with 10% normal donkey serum prepared in 1% bovine serum albumin (BSA) in PBS for 20 minutes to suppress non-specific IgG binding. Primary antibody (rat anti-A6; 1:100, gift from Dr. Valentina Factor) was prepared in 1% BSA in PBS and applied to sections for 1 hour at room temperature. Following washing with PBS, sections were incubated in the dark with Alexa 488-conjugated donkey anti-rat secondary antibody in 1% BSA in PBS for 1 hour. Following washing with PBS, sections were counterstained and mounted using ProLong Gold antifade reagent (Thermo Fisher) or Gelvatol. Fluorescent microscopy was performed on a Zeiss Axioscope microscope. Representative photomicrographs are shown.

Protein extraction, cell fractionation, immunoprecipitation, and Western blots:

Protein lysates were prepared as previously described (10). Briefly, whole-cell lysates from mouse livers or cell lysates from hepatoma cell lines were prepared by homogenizing in radioimmunoprecipitation assay (RIPA) buffer containing Halt protease inhibitor cocktail. Nuclear extracts were prepared using the NE-PER

Nuclear and Cytoplasmic Extraction Reagents kit as per the manufacturer's instructions (Thermo Fisher Scientific, Rockford, IL). The concentration of protein in all lysates was determined by the bicinchoninic acid assay using bovine serum albumin as a standard.

Immunoprecipitation (IP) was performed on 750-1000µg of whole liver lysate or 500µg cell lysate (all prepared in RIPA buffer in the presence of inhibitors), which was first precleared with species-specific IgG and Protein A/G agarose for 30 minutes at 4°C. After centrifugation, the supernatants were incubated with 18µl FXR antibody (rabbit H-130) (Santa Cruz Biotechnology) overnight at 4°C. The next day, samples were incubated with Protein A/G agarose for 1 hour at 4°C. Alternatively, precleared supernatants were incubated with 18µl agarose-conjugated goat anti-β-catenin antibody for 2.5 hours at room temperature. Pellets from all immunoprecipitation studies were collected, washed in PBS containing inhibitors, resuspended in loading buffer, and subjected to electrophoresis, as described below.

Sodium dodecyl sulfate-polyacrylamide gel electrophoresis (SDS-PAGE) analysis was performed with 20µg or 50µg of protein or 20 µl of eluate from IP complexes and resolved on Bio-Rad Protean precast gels under reducing conditions, followed by transfer to polyvinylidene difluoride membranes (PVDF, Millipore, Bedford, MA) membrane. Membranes were stained with Ponceau-S solution to confirm equal loading and then blocked in 5% milk, followed by

incubation with primary antibody in 5% milk overnight at 4°C. Primary antibodies used include β-catenin (1:500, BD Biosciences, San Jose, CA), glutamine synthetase (1:800), RXRα (1:200), FXR (1:500; all from Santa Cruz Biotechnology), and β-actin (1:5000, Chemicon). Membranes were then incubated with appropriate horseradish-peroxidase conjugated secondary antibodies (Chemicon) at concentrations of 1:25,000 to 1:50,000 in 1% milk for 1 hour at room temperature followed by washing. Proteins were detected by Super-Signal West Pico Chemiluminescent Substrate (Pierce) and visualized by autoradiography. Blots were stripped with Restore buffer (Pierce) for 10 minutes before re-probing. Representative blots are presented.

RNA isolation and real-time PCR:

RNA was extracted from WT and β-catenin KO livers of sham-operated and BDL mice, Hep3B cells treated with either control siRNA or RXRα siRNA, or C57BL/6 mice treated with either EZN-3892 β-catenin antisense LNA ASO or EZN-3046 control LNA ASO using Trizol (Invitrogen). RNA was DNase-treated and equal microgram amounts of RNA from each sample were used to make individual cDNA samples with SuperScript III First –Strand Synthesis System for RT-PCR (Invitrogen). cDNA along with 1x Power SYBR-Green PCR Master Mix (Applied Biosystems) and the appropriate primers (Supplemental Tables 1 and 2) were used for each real-time PCR reaction. The Applied Biosystems StepOnePlus Real-Time PCR System was used for the analysis of the transcripts with the StepOne v2.1 software. The comparative ΔΔCT method was used for analysis of

the data and all data is presented normalized to either sham WT, control siRNA, scrambled ASO, or control PBS. 18sRNA expression was used as the internal control for WT and β-catenin KO livers, mouse GAPDH was used as the internal control for the ASO-treated livers and control PBS-treated livers, and human β-actin primers were used as the internal control for Hep3B cells.

DNA isolation and genomic PCR:

DNA was extracted from WT and FXR KO livers using the REDExtract-N-Amp Tissue PCR kit (Sigma). Genotyping was performed as described previously using the following primers (11):

F1: 5'-TCTCTTTAAGTTGATGACGGGAATCT-3'

F2: 5'-GCTCTAAGGAGAGTCACTTGTGCA-3'

R1: 5'-GCATGCTCTGTTCATAAACGCCAT-3.

Primers F1/R1 produce a 249 bp wild-type (unrecombined) product, while primers F2/R1 produce a 291 bp deleted (recombined) product.

Locked nucleic acid antisense oligonucleotide therapeutic intervention:

C57BL/6 mice were subjected to BDL as above. Seven days before BDL, 5 animals received one intraperitoneal (i.p.) injection of EZN-3892 β-catenin antisense LNA ASO (Santaris Pharma A/S) at 15 mg/kg. Four animals received EZN-3046 scrambled LNA ASO at the same concentration. Subsequent doses of

EZN-3892 or EZN-3046 were administered every 48 hours for two weeks (11 injections total). All mice were sacrificed at day 12 after BDL. Livers from the control and experimental groups were utilized for IHC, IF, total BA, IP, and Western blotting as above.

Therapeutic intervention with β-catenin RNAi targeted to hepatocytes:

C57BL/6 mice were subjected to BDL as above. Three days before BDL, 5 animals received one subcutaneous injection of β-catenin RNAi agent conjugated to N-acetylgalactosamine (GalXC; Dicerna Pharmaceuticals) at 5 mg/kg. Five animals received PBS subcutaneously at the same volume. After BDL, animals were dosed weekly thereafter with either PBS or GalXC-CTNNB1 until the time of sacrifice (day 14 after BDL). Livers from the control and experimental groups were utilized for IHC, IF, total BA, IP, and Western blotting as above.

Measurement of bile acid composition:

Liver samples were homogenized in water (100 mg tissue in 400 mL water), and then a 200 mL aliquot of methanol was added to 100 mL of liver homogenate. The mixture was vortexed twice for 1 min and centrifuged at 15,000xg for 20 minutes. Bile from gallbladders was dissolved in acetonitrile:H2O (1:1; 2 µL in 1000 µL), vortexed for 30 seconds, and centrifuged at 15,000xg. One microliter of the supernatants from all samples were injected onto the ultra-performance

liquid chromatography and quadrupole time-of-flight mass spectrometry (UPLC–QTOFMS) for analysis as described previously (12, 13).

Characterization of the SHP/Nr0b2 region in normal mouse liver:

ChIPseq studies of RXRα, FXR, TCF4, H4K5Ac (transcriptionally active chromatin), and H3K4Me3 (active promoter regions) were aligned with RNAseq reads to identify binding regions. Data is derived from a manuscript in preparation by Tian and Locker; the FXR analysis is described in (14).

Statistics:

All experiments were performed with 3-9 animals within each group. Serum biochemistry, total bile acid measurements, and real-time PCR data were compared for statistical analysis by Student t test (Excel) and p-value of less than 0.05 was considered significant. Densitometry analyses and quantification of Sirius Red, TUNEL, and A6 staining were performed using ImageJ software (version 1.44o).

Study approval:

All animal experiments were performed under the guidelines of the National Institutes of Health and the Institutional Animal Use and Care Committee at the University of Pittsburgh. The studies performed in the current report were

approved by the Institutional Animal Use and Care Committee at the University of Pittsburgh (protocol #14013027).

REFERENCES

1. Apte U, Thompson MD, Cui S, Liu B, Cieply B, Monga SP. Wnt/beta-catenin signaling mediates oval cell response in rodents. Hepatology 2008;47:288-295.
2. Schmidt DR, Schmidt S, Holmstrom SR, Makishima M, Yu RT, Cummins CL, Mangelsdorf DJ, et al. AKR1B7 is induced by the farnesoid X receptor and metabolizes bile acids. J Biol Chem 2011;286:2425-2432.
3. Seok S, Fu T, Choi SE, Li Y, Zhu R, Kumar S, Sun X, et al. Transcriptional regulation of autophagy by an FXR-CREB axis. Nature 2014;516:108-111.
4. Guo GL, Santamarina-Fojo S, Akiyama TE, Amar MJ, Paigen BJ, Brewer B, Jr., Gonzalez FJ. Effects of FXR in foam-cell formation and atherosclerosis development. Biochim Biophys Acta 2006;1761:1401-1409.
5. Nejak-Bowen K, Kikuchi A, Monga SP. Beta-catenin-NF-kappaB interactions in murine hepatocytes: a complex to die for. Hepatology 2013;57:763-774.
6. Li G, Thomas AM, Hart SN, Zhong X, Wu D, Guo GL. Farnesoid X receptor activation mediates head-to-tail chromatin looping in the Nr0b2 gene encoding small heterodimer partner. Mol Endocrinol 2010;24:1404-1412.
7. Emami KH, Nguyen C, Ma H, Kim DH, Jeong KW, Eguchi M, Moon RT, et al. A small molecule inhibitor of beta-catenin/CREB-binding protein transcription [corrected]. Proc Natl Acad Sci U S A 2004;101:12682-12687.
8. Lee JM, Yang J, Newell P, Singh S, Parwani A, Friedman SL, Nejak-Bowen KN, et al. beta-Catenin signaling in hepatocellular cancer: Implications in inflammation, fibrosis, and proliferation. Cancer Lett 2014;343:90-97.
9. Thompson MD, Awuah P, Singh S, Monga SP. Disparate cellular basis of improved liver repair in beta-catenin-overexpressing mice after long-term exposure to 3,5-diethoxycarbonyl-1,4-dihydrocollidine. Am J Pathol 2010;177:1812-1822.
10. Nejak-Bowen K, Orr A, Bowen WC, Jr., Michalopoulos GK. Conditional genetic elimination of hepatocyte growth factor in mice compromises liver regeneration after partial hepatectomy. PLoS One 2013;8:e59836.
11. Sinal CJ, Tohkin M, Miyata M, Ward JM, Lambert G, Gonzalez FJ. Targeted disruption of the nuclear receptor FXR/BAR impairs bile acid and lipid homeostasis. Cell 2000;102:731-744.
12. Liu K, Yan J, Sachar M, Zhang X, Guan M, Xie W, Ma X. A metabolomic perspective of griseofulvin-induced liver injury in mice. Biochem Pharmacol 2015;98:493-501.
13. Jiang C, Xie C, Li F, Zhang L, Nichols RG, Krausz KW, Cai J, et al. Intestinal farnesoid X receptor signaling promotes nonalcoholic fatty liver disease. J Clin Invest 2015;125:386-402.
14. Thomas AM, Hart SN, Kong B, Fang J, Zhong XB, Guo GL. Genome-wide tissue-specific farnesoid X receptor binding in mouse liver and intestine. Hepatology 2010;51:1410-1419.

Supplemental Table 1: Primers used for real-time PCR studies on WT and β-catenin KO mouse livers

Gene	**Forward Primer**	**Reverse Primer**
Cyp7a1	TGGGCATCTCAAGCAAACAC	TCATTGCTTCAGGGCTCCTG
Cyp8b1	GCCCTTACTCCAAATCCTACCA	TCGCACACATGGCTCGAT
Cyp27	TGCCTGGGTCGGAGGAT	GAGCCAGGGCAATCTCATACTT
Cyp2b10	CAATGGGGAACGTTGGAAGA	TGATGCACTGGAAGAGGAAC
Cyp3a11	CCACCAGTAGCACACTTTCC	TTCCATCTCCATCACAGTATCA
NTCP	CACCATGGAGTTCAGCAAGA	AGCACTGAGGGGCATGATAC
OATP4	GATCCTTCACTTACCTGTTCAA	CCTAAAAACATTCCACTTGCCATA
BSEP	GAGTGGTGGACAGAAGCAAA	TGAGGTAGCCATGTCCAGAA
MRP2	GCTTCCCATGGTGATCTCTT	ATCATCGCTTCCCAGGTACT
MRP3	TGAGATCGTCATTGATGGGC	AGCTGAGAGCGCAGGTCG
MRP4	TTAGATGGGCCTCTGGTTCT	GCCCACAATTCCAACCTTT
FXR	TGGGCTCCGAATCCTCTTAGA	TGGTCCTCAAATAAGATCCTTGG
SHP	TCTGCAGGTCGTCCGACTATTC	AGGCAGTGGCTGTGAGATGC
PXR	CCCATCAACGTAGAGGAGGA	GGGGGTTGGTAGTTCCAGAT
FGFR4	ACCAACACTGGAGCCTGGT	AGGAGATAGCTGTAGCGAATGC
GAPDH	ACCCAGAAGACTGTGGATGG	CACATTGGGGGTAGGAACAC
18sRNA	GTAACCCGTTGAACCCCATT	CCATCCAATCGGTAGTAGCG

Supplemental Table 2: Primers used for real-time PCR studies on Hep3B hepatoma cells

Gene	**Forward Primer**	**Reverse Primer**
RXRα	TCAATGGCGTCCTCAAGGTC	TTGCCTGAGGAGCGGTCC
β-actin	CCATCGAGCACGGCATC	ATTGTAGAAGGTGTGGTGCCAGA

Supplemental Table 3: Primers used for ChIP assay on WT and β-catenin KO mouse livers

Gene	**Forward Primer**	**Reverse Primer**
SHP	GCATCAATAGAAACAGCAGTCCCAAGGCA	CACAGGGCCACCTGCCCACTGCCT

Supplemental Table 4: Primers used for ChIP assay on Hep3B cells

Gene	**Forward Primer**	**Reverse Primer**
SHP	CAGTCCACGCCCTCAGCCC	GGCAGGAGGAGGTCTGAAAGC
Ostβ	GAAAGTCAGGTGGAGCCTGTTTGCACT	ACCCATCTGGTAGCTCTGGCCTTAGCAC

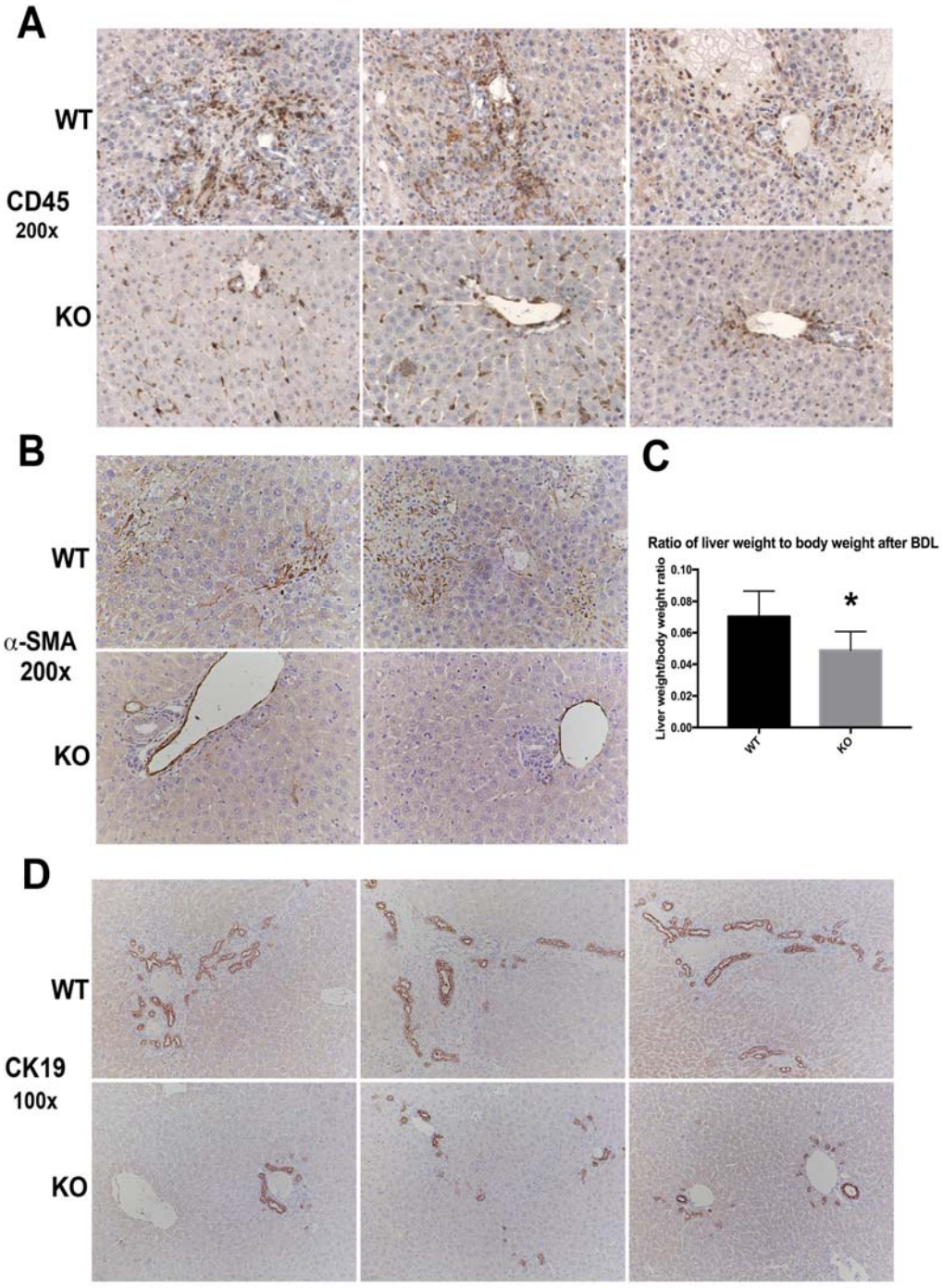
A
WT
CD45
200x
KO
B
WT
α-SMA
200x
KO
C
Ratio of liver weight to body weight after BDL
Liver weight/body weight ratio
0.10
0.08
0.06
0.04
0.02
0.00
*
WT
KO
D
WT
CK19
100x
KO

Supplemental Figure 1: Decreased inflammation, fibrosis, and ductular reaction in KO following BDL. (A) IHC shows fewer CD45+ inflammatory cells especially in the periportal region. (B) α-SMA-positive cells were evident around the bile duct mass in WT after BDL, while they were conspicuously absent in KO. (C) Liver weight to body weight ratios are decreased in KO compared to WT after BDL. (D) IHC for CK19 shows notably fewer bile ducts in KO after BDL as compared to WT.

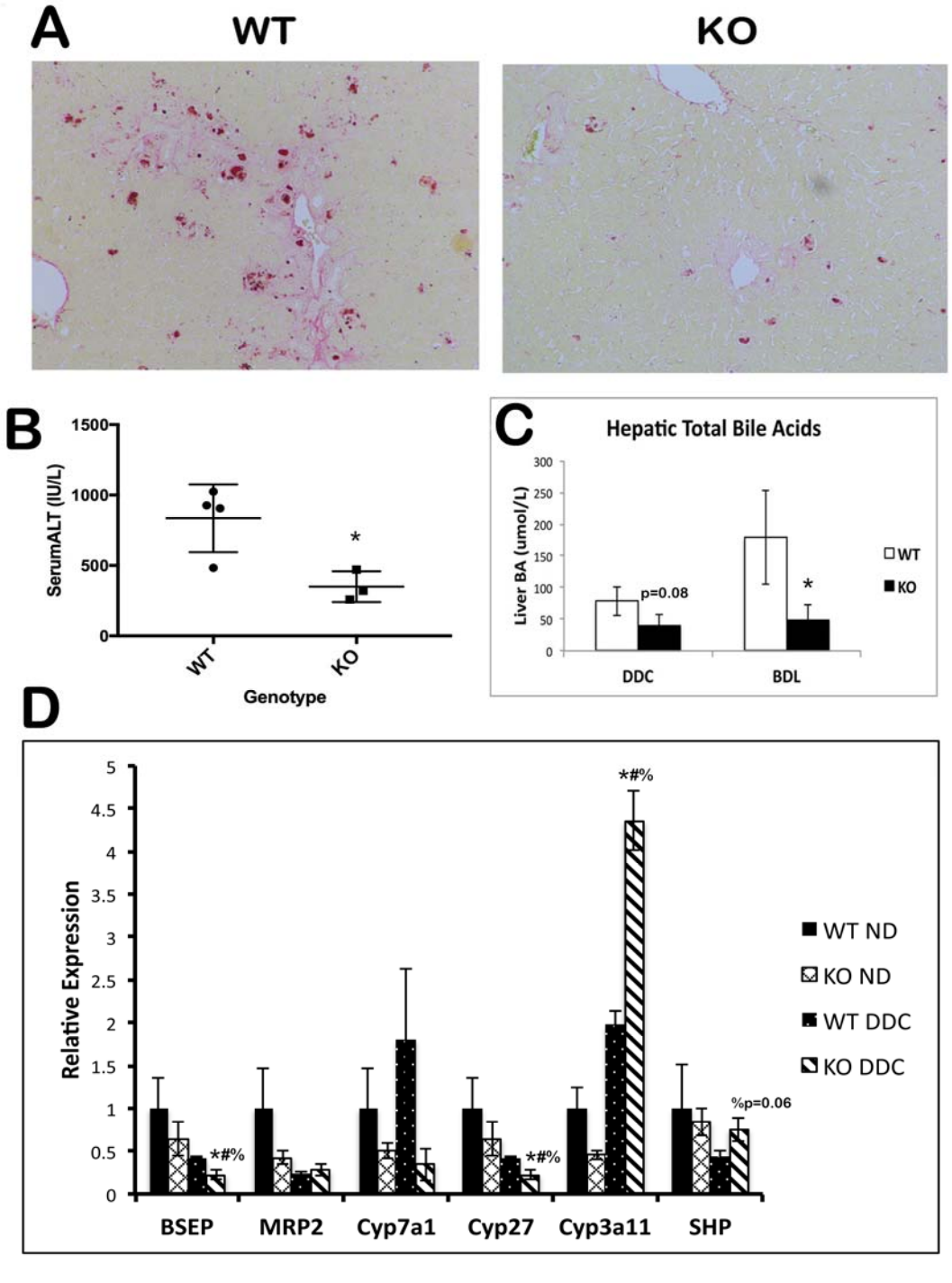
A
WT
KO
B
SerumALT (IU/L)
1500
1000
500
0
*
WT
KO
Genotype
C
Hepatic Total Bile Acids
Liver BA (umol/L)
300
250
200
150
100
50
0
p=0.08
*
WT
KO
DDC
BDL
D
Relative Expression
5
4.5
4
3.5
3
2.5
2
1.5
1
0.5
0
*#%
*#%
*#%
%p=0.06
WT ND
KO ND
WT DDC
KO DDC
BSEP
MRP2
Cyp7a1
Cyp27
Cyp3a11
SHP

Supplemental Figure 2: Decreased injury, fibrosis, and BA synthesis in β-catenin KO after short-term DDC diet. (A) KO had significantly less fibrosis than WT after 28 days of DDC diet, as assessed by Sirius red staining (100x). (B) Decreased ALT in KO at 28 days after DDC when compared to the WT (n=3-4 per group). (C) Insignificant decrease in total BA in KO after 28 days of DDC diet. Note the modest increase in total BA after DDC, compared to that seen after BDL. *$p<0.05$. (D) BSEP and MRP2 are not increased in KO after 28 days of DDC diet. Cyp7a1 and Cyp27 expression is decreased, while Cyp3a11 expression is increased, in KO after DDC diet. SHP expression is insignificantly increased in KO after DDC diet. *$p<0.05$ vs. control diet WT, #$p<0.05$ vs. control diet KO, %$p<0.05$ vs. DDC WT.

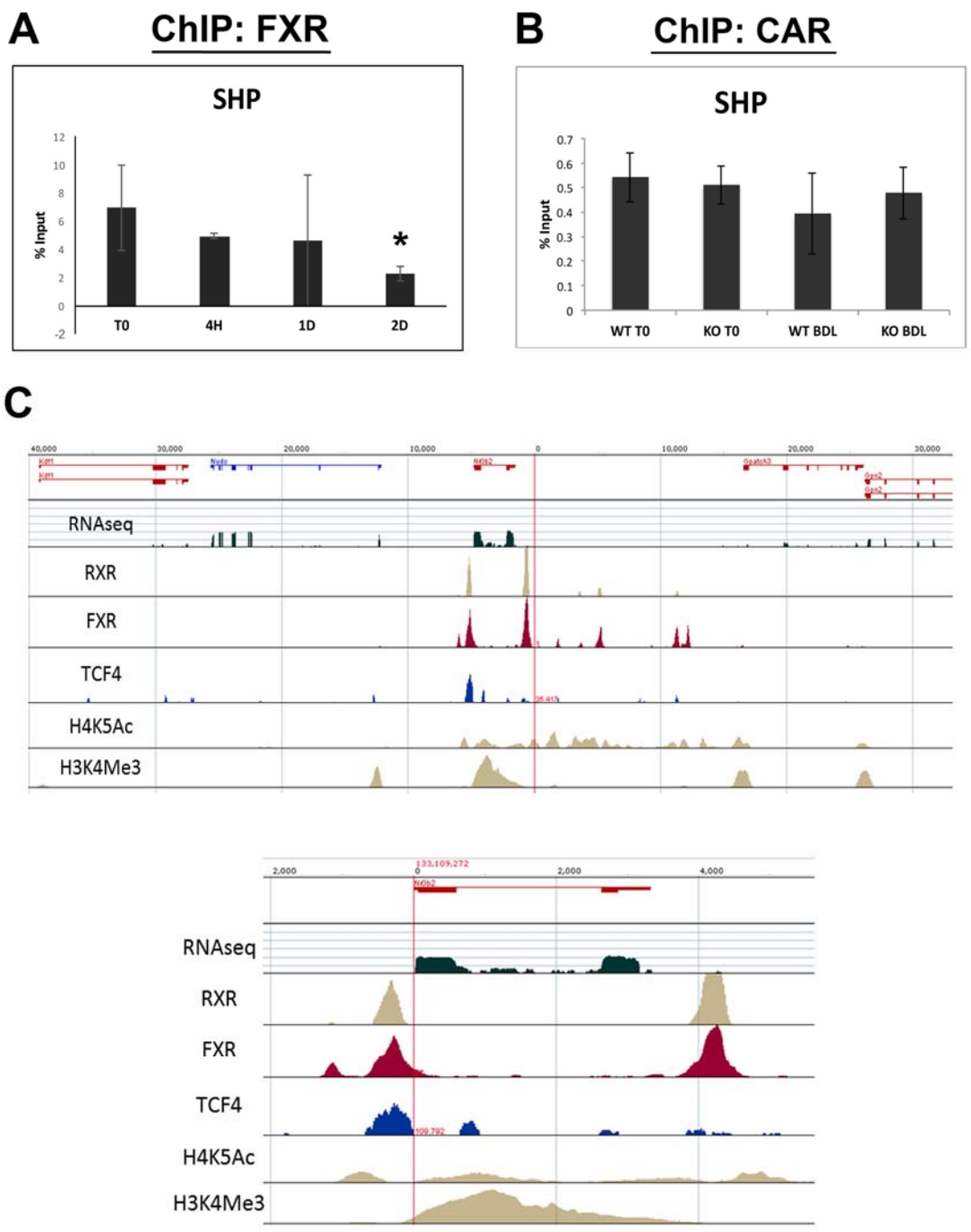
A
ChIP: FXR
SHP
% Input
12
10
8
6
4
2
0
-2
T0
4H
1D
2D
*
B
ChIP: CAR
SHP
% Input
0.7
0.6
0.5
0.4
0.3
0.2
0.1
0
WT T0
KO T0
WT BDL
KO BDL
C
RNAseq
RXR
FXR
TCF4
H4K5Ac
H3K4Me3
RNAseq
RXR
FXR
TCF4
H4K5Ac
H3K4Me3

Supplemental Figure 3: FXR and RXRα occupancy of the SHP promoter in KO after 14D BDL is specific, and the SHP promoter also contains a TCF4 binding site. (A) ChIP assay for FXR shows lack of increase in SHP occupancy at early time points after BDL in WT. *p<0.05. (B) ChiP for CAR shows no change in SHP promoter occupancy in WT or KO before or after BDL. (C) ChIP-seq studies of RXRα, FXR, TCF4, H4K5Ac (transcriptionally active chromatin), and H3K4Me3 (active promoter regions) are aligned with RNAseq reads. FXR, RXRα, and TCF4 all bind to an enhancer near the SHP promoter. These factors also bind to other enhancers in the region, all associated with SHP. Top: ChIP-seq map across a 40,000 bp region of the SHP/Nr0b2 promoter showing binding sites for FXR, RXRα, and TCF4 relative to the transcription start site as well as histone acetylation and methylation of the transcribed region. Bottom: close capture focusing on the peaks of FXR, RXRα, and TCF4 binding in the enhancer region of the SHP promoter.

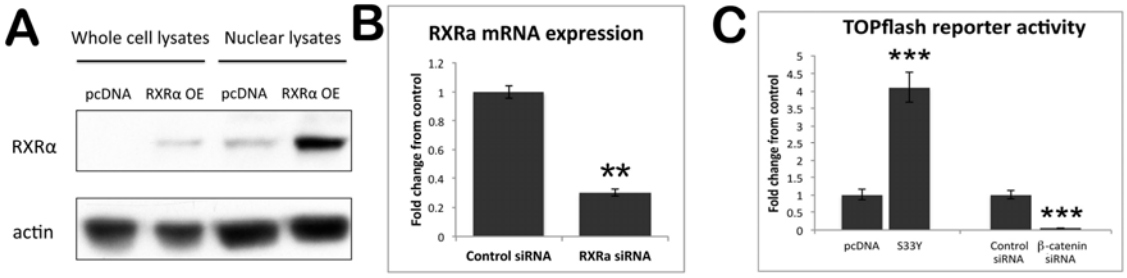
A
Whole cell lysates
Nuclear lysates
pcDNA
RXRα OE
pcDNA
RXRα OE
RXRα
actin
B
RXRa mRNA expression
Fold change from control
1.2
1
0.8
0.6
0.4
0.2
0
**
Control siRNA
RXRa siRNA
C
TOPflash reporter activity
Fold change from control
5
4.5
4
3.5
3
2.5
2
1.5
1
0.5
0
***
***
pcDNA
S33Y
Control siRNA
β-catenin siRNA

Supplemental Figure 4: Confirmation of efficient knockdown and overexpression of β-catenin and RXRα expression for co-IP studies. (A) RXRα overexpression in Hep3B cells increases RXRα protein expression in whole cell lysates and nuclear lysates. (B) RXRα siRNA suppresses mRNA expression in Hep3B cells. (C) TOPflash reporter demonstrates β-catenin siRNA suppresses β-catenin/TCF4 activation in Hep3B cells, while cells transfected with S33Y mutated constitutively active β-catenin show increased β-catenin/TCF4 activity. **p<0.01; ***p<0.001.

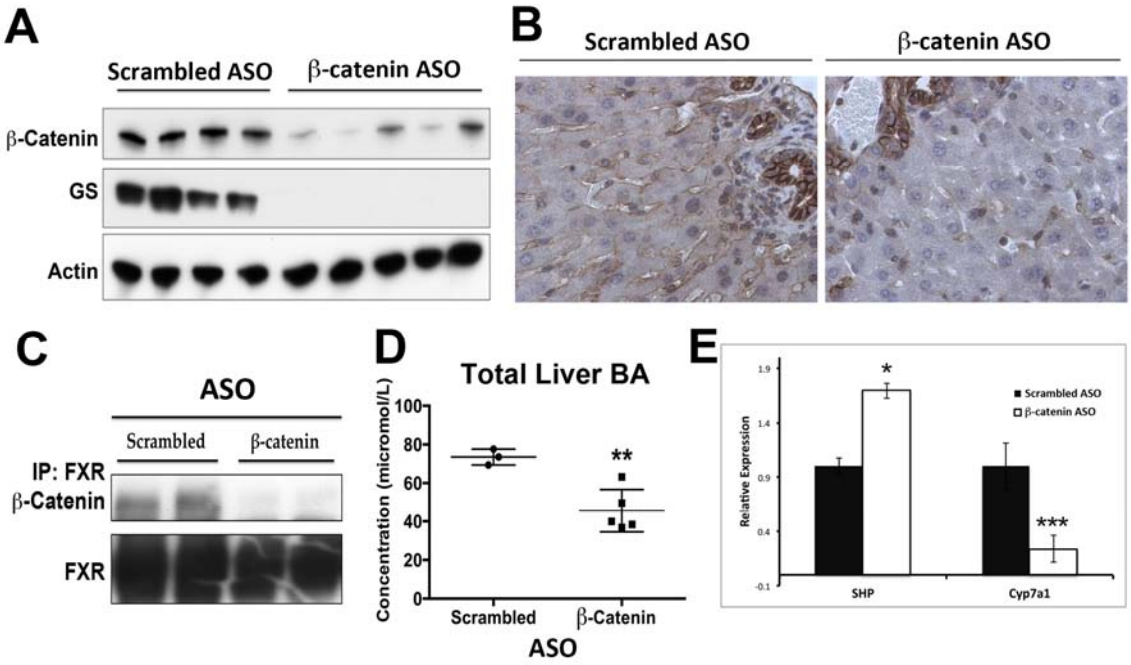
A
Scrambled ASO
β-catenin ASO
β-Catenin
GS
Actin
B
Scrambled ASO
β-catenin ASO
C
ASO
Scrambled
β-catenin
IP: FXR
β-Catenin
FXR
D
Total Liver BA
Concentration (micromol/L)
100
80
60
40
20
0
**
Scrambled
β-Catenin
ASO
E
Relative Expression
1.9
1.4
0.9
0.4
-0.1
*
***
Scrambled ASO
β-catenin ASO
SHP
Cyp7a1

Supplemental Figure 5: β-catenin suppression by LNA ASO treatment results in less β-catenin/FXR complex and reduced BA after BDL. (A) WB shows successful decrease in β-catenin and GS protein after β-catenin but not scrambled ASO treatment after BDL. (B) IHC shows the presence of membranous and nuclear β-catenin in hepatocytes and cholangiocytes of scrambled ASO-treated mice after BDL, while after β-catenin ASO treatment β-catenin is found only in cholangiocytes (400x). (C) IP shows decreased FXR/β-catenin association after β-catenin ASO treatment. (D) Liver TBA are decreased in β-catenin ASO-treated livers. (E) Expression of direct FXR target SHP is significantly increased in β-catenin ASO- treated livers after BDL, while indirect target Cyp7a1 is suppressed. *p<0.05; **p<0.01; ***p<0.001.

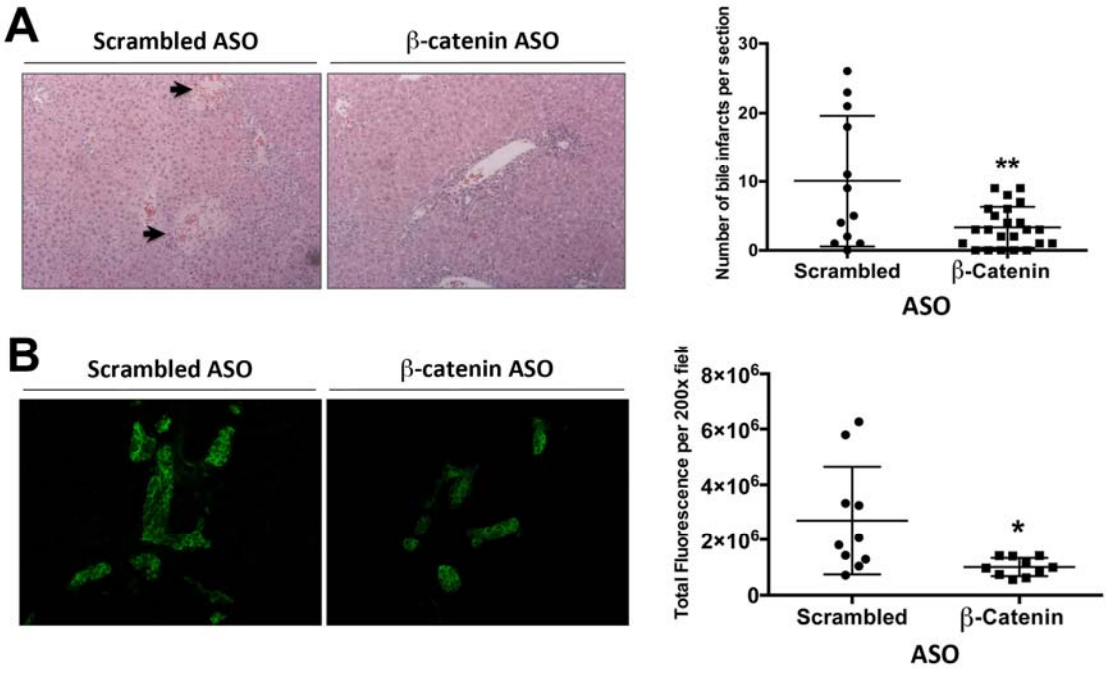
A
Scrambled ASO
β-catenin ASO
Number of bile infarcts per section
30
20
10
0
**
Scrambled
β-Catenin
ASO
B
Scrambled ASO
β-catenin ASO
Total Fluorescence per 200x fiel
8×10^6
6×10^6
4×10^6
2×10^6
0
*
Scrambled
β-Catenin
ASO

Supplemental Figure 6: Decrease in liver injury and ductular proliferation in mice treated with β-catenin ASO after BDL. (A) H&E shows fewer bile infarcts (arrows) in β-catenin ASO-treated livers after BDL (200x; left panel). Quantification of bile infarcts after ASO treatment and BDL shows significantly fewer infarcts in β-catenin ASO group (right panel). For A, 4-5 representative lobes per animal (n=3 scrambled ASO; n=5 β-catenin ASO) were quantified. **p<0.01. (B) IF for A6 shows decreased ADP in β-catenin ASO-treated livers after BDL as compared to scrambled ASO (200x; left panel). Quantification of total fluorescence per field in A6-stained livers after ASO treatment and BDL shows significantly less ductular proliferation in β-catenin ASO group (right panel). n=3 images per 3 representative animals per group were quantified. *p<0.05.

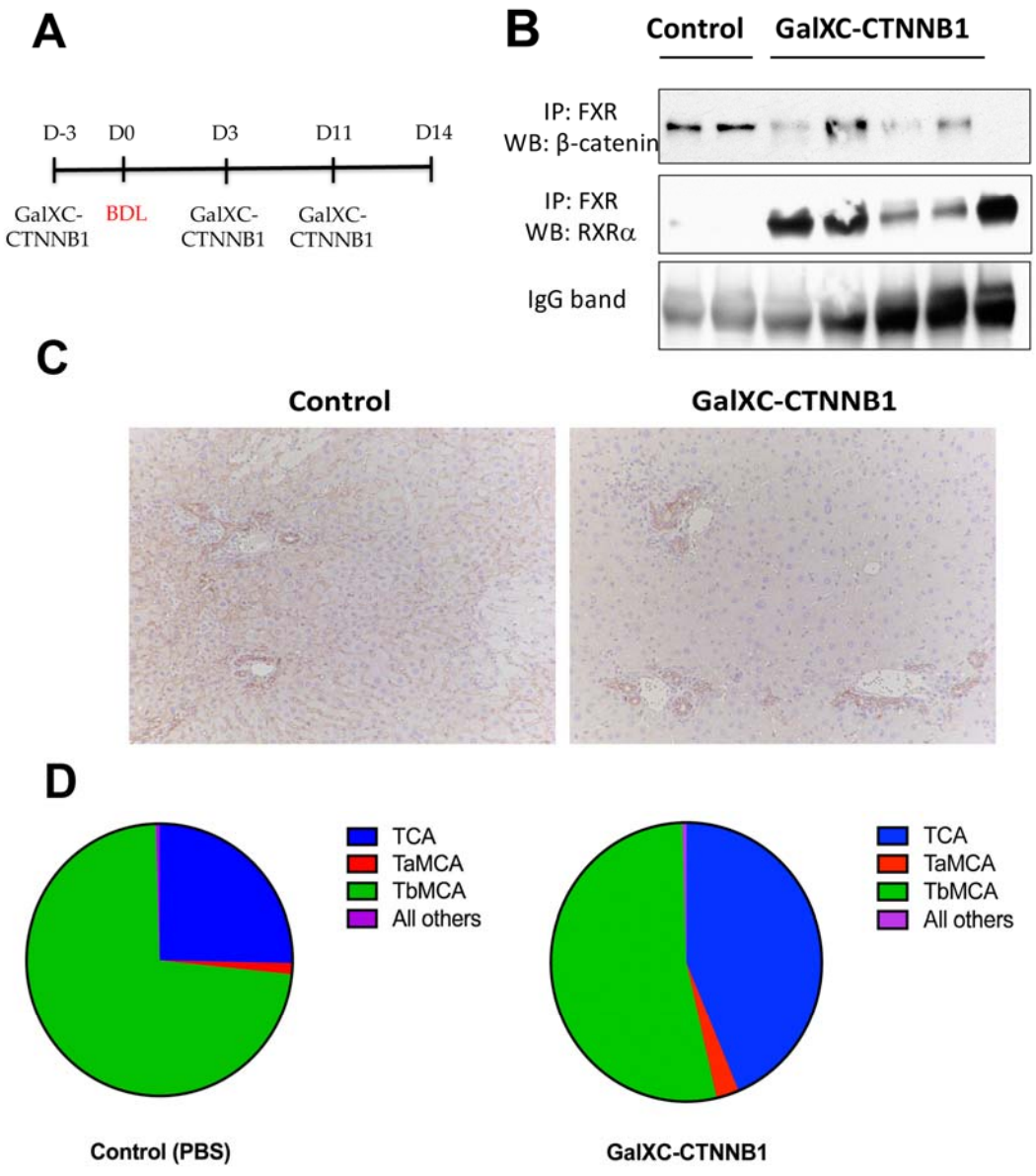
A
D-3
D0
D3
D11
D14
GalXC-CTNNB1
BDL
GalXC-CTNNB1
GalXC-CTNNB1
B
Control
GalXC-CTNNB1
IP: FXR
WB: β-catenin
IP: FXR
WB: RXRα
IgG band
C
Control
GalXC-CTNNB1
D
TCA
TaMCA
TbMCA
All others
Control (PBS)
TCA
TaMCA
TbMCA
All others
GalXC-CTNNB1

Supplemental Figure 7: Decrease in FXR/β-catenin association and changes in BA composition in mice treated with GalXC-CTNNB1 after BDL. (A) Schematic of the GalXC-CTNNB1 study, in which mice were treated with PBS or 5 mg/kg β-catenin DsiRNA conjugated to GalXC (GalXC-CTNNB1), followed by BDL 3 days later, and then weekly doses of either PBS or 5 mg/kg GalXC-CTNNB1 for the duration of the experiment. Mice were harvested 14 days following BDL. (B) IP shows decreased FXR/β-catenin association after GalXC-CTNNB1 treatment and BDL, while FXR/RXRα association increases. (C) IHC shows the presence of β-catenin in hepatocytes and cholangiocytes of control mice after BDL, while after GalXC-CTNNB1 treatment β-catenin is found only in cholangiocytes (100x). (D) Analysis of BA species in gallbladder shows lesser TβMCA in bile of GalXC-CTNNB1-treated mice when expressed qualitatively as a percentage of total BA.

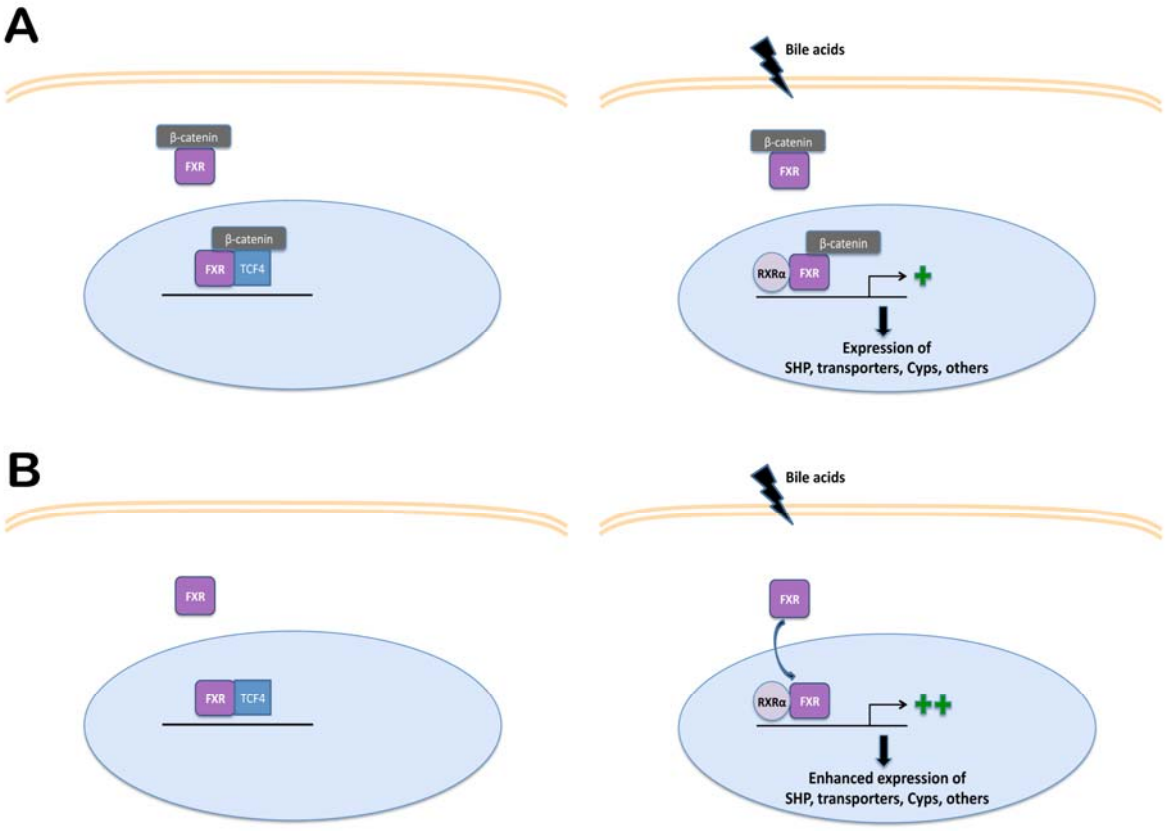
A
β-catenin
FXR
β-catenin
FXR
TCF4
Bile acids
β-catenin
FXR
β-catenin
RXRα
FXR
Expression of
SHP, transporters, Cyps, others
B
FXR
FXR
TCF4
Bile acids
FXR
RXRα
FXR
Enhanced expression of
SHP, transporters, Cyps, others

Supplemental Figure 8: Schematic for the role of β-catenin in regulating FXR activity during cholestasis. (A) In WT mice, β-catenin is associated with FXR; this association is hypothesized to occur in both the cytoplasm and in the nucleus, where a fraction of FXR is bound to the promoter region of various target genes, including SHP. TCF4, which also binds to the SHP promoter, is also present. In the presence of BA, TCF4 binding decreases, RXRα/FXR heterodimers are formed, and transcription of downstream targets occurs resulting in suppressed BA synthesis and altered transport. (C) In β-catenin KO mice, loss of inhibitory β-catenin/FXR complex results in increased basal activity of SHP promoter as demonstrated by H4K5 ChIP, which may in turn activate a negative feedback loop that maintains homeostasis. Absence of the FXR/β-catenin complex also results in earlier and/or increased nuclear translocation of FXR in the presence of BA, which simultaneously triggers loss of TCF4 binding to the SHP promoter. Together, the net result of these modifications is enhanced activation of FXR, increased expression of downstream targets, and optimal reduction and alteration of the hepatic BA pool during cholestasis.